INTERNATIONAL JOURNAL OF INTEGRATED ENGINEERING
ISSN: 2229-838X e-ISSN: 2600-7916

IJIE

Vol. 16 No. 9 (2024) 264-272
https://publisher.uthm.edu.my/ojs/index.php/ijie

Numerical Optimization of Plasmonic CuO-Based Semi-Transparent Thin Film Solar Cell Device via L9 Taguchi Orthogonal Array Method and ANOVA

J. Husna[1,3], N.A. Jamil[1], K.S. Siow[1], T. R. Lenka[4], H. Kumar[5], P. Chelvanathan[2], M. A. Mohamed[1], A.R. Zain[1], J. Sampe[1], P. S. Menon[1]*

[1] *Institute of Microengineering and Nanoelectronics (IMEN), Universiti Kebangsaan Malaysia (UKM), Bangi, 43600, MALAYSIA*
[2] *Solar Energy Research Institute (SERI), Universiti Kebangsaan Malaysia (UKM), Bangi, 43600, MALAYSIA*
[3] *Department of Electrical Engineering, Islamic University of North Sumatra, Sumatera Utara, 20217, INDONESIA*
[4] *Department of Electronics and Communication Engineering, National Institute of Technology Silchar, INDIA*
[5] *Department of Electronics and Communication Engineering, The LNM Institute of Information Technology, INDIA*

*Corresponding Author: susi@ukm.edu.my
DOI: https://doi.org/10.30880/ijie.2024.16.09.021

Article Info

Received: 6 April 2024
Accepted: 24 November 2024
Available online: 29 December 2024

Keywords

Semi-transparent, thin film solar cell, copper oxide, Taguchi L9, zinc oxide, SCAPS-1D, plasmonic

Abstract

The future of smart cities and energy-efficient infrastructures are very much dependent on photovoltaic materials that are sustainable, functional and affordable. In this context, copper oxide (CuO)-based solar cells provide the advantages of energy harvesting coupled with semi-transparent light transmission. In this work, a p-CuO thin film layer was used together with n-doped zinc oxide (ZnO), Al-doped zinc oxide (AZO) and indium tin oxide (ITO) to form a semi-transparent thin film solar cell (STFSC) model developed using SCAPS-1D and optimized using Taguchi L9 orthogonal array and analysis of variance (ANOVA). Optimized parameters for the CuO absorber and ZnO window/buffer layers were obtained for the best values for doping variation level and layer thickness. With the optimized design parameters, the performance of the STFSC device was improved in terms of the open circuit voltage (Voc), short circuit current (Jsc), fill factor (FF) and efficiency (η). Furthermore, the power conversion efficiency (PCE) of the STFSC device with and without CuO plasmonic nanoparticles correspond to 10.27 % and 15.57 % respectively. The increased light absorption was due to the effect of the larger surface area of the CuO plasmonic nanoparticles in the p-CuO absorber layer which increased light absorption and subsequently increasing the photocurrent.

1. Introduction

Building-integrated photovoltaics (BIPV) such as semi-transparent thin film solar cells (STFSC) are in-line with several United Nations Sustainable Development Goals (SDGs) such as SDG 7: Affordable and Clean Energy, SDG 11: Sustainable Cities and Communities, SDG 9: Industry, Innovation, and Infrastructure and SDG 13: Climate Action. This is because STSFC provides decentralized, clean power directly within buildings, reduces reliance on

fossil fuels, promotes energy-efficient infrastructure, reduces greenhouse gas emissions and mitigates climate change [1].

Recently, transition metal dichalcogenides (TMDCs) have received high attention to become potential candidates instead of traditional materials for various applications especially for solar cells, as well as batteries, photodetectors, biomedical, and catalysis. In these materials, the d-d transition positioned at a metal site produces large band-edge excitation and therefore unique electronic properties leading to its suitability for various applications [2]. Among the TMDC materials, copper oxide (CuO) is a promising material in several applications, including in photovoltaic cells such as STFSCs [3]. It is a suitable absorber layer in solar cells due to its good absorbance and electrical conductivity [4-6]. In addition, it has low toxicity and low electrical resistivity and is recognized for being a cost-effective material. The CuO bandgap ranges from 1.2 to 1.9 eV, as reported in previous work [7, 8]. Furthermore, CuO is thermally resistant due to its high oxidation state, which improves its performance in varying environmental conditions. Thermal stability is essential for the efficiency of solar cells as overheating may reduce conductivity and degrade overall performance [9].

Typically, CuO is used as a p-type semiconductor in solar cell devices and it is coupled with n-type semiconductors such as zinc oxide (ZnO) and some other materials [10, 11]. Moreover, both metal oxides (CuO and ZnO) have been applied as absorbers and window/buffer layers in semi-transparent solar cell devices [11]. Our previous work [12] involved the development of p-CuO/n-ZnO/AZO/ITO STFSC device model employing Solar Cell Capacitance Simulator Structures (SCAPS-1D) software, which is a one-dimensional (1D) windows-oriented program and has the largest number of simulation parameters. In this work, we optimize the device parameters using the Taguchi L9 orthogonal array method. Optimizing the absorber layer comprising of CuO and ZnO thin films has the potential to significantly improve power conversion efficiency (PCE), a key factor for the successful development of these devices [13-15].

Taguchi method has been used widely in research institutions and companies to improve productivity during research and development phases. This method utilizes an orthogonal array (OA) design to study various factors affecting performance results while reducing the required number of the experimental trials [16]. By minimizing the number of parameters used in device simulation, thereby it also saves cost and time [17]. Taguchi method is known as economical in characterizing multivariable processes since it uses fewer experiments and simulations to optimize the levels of various parameters. Theoretically, this technique can determine the experimental condition having less variability, which can be expressed by the signal-to-noise (S/N) ratio, as the optimum condition. In addition, this method is also usually utilized to investigate or evaluate the relationship between one or more response variables and a set of quantitative experimental or simulation variables or factors. In addition to theTaguchi method, Analysis of Variance (ANOVA) is an effective statistical tool for assessing the optical and electrical properties of the CuO and ZnO films used in the device model. ANOVA allows for the identification of factors that substantially impact performance metrics such as PCE, causing subsequent improvements based on empirical findings [18-23].

2. Materials and Method

The previous CuO-based STFSC device was developed using numerical modeling software SCAPS-1D. In this work, the developed device parameters were optimized using Taguchi method and ANOVA. Subsequently, the newly optimized devices parameters were used to simulate the device again using SCAPS-1D. Plasmonic effects utilizing CuO nanoparticles were also simulated.

2.1 Numerical Modeling

SCAPS-1D (version 3.3.0.) software was used to simulate the CuO-based STFSC device Fig. 1(a) shows the CuO-based STFSC device structure whereas Fig. 1(b) portrays the comparison of the absorption coefficient of CuO thin film versus CuO nanoparticles when used as the absorber layer in the STFSC device. CuO nanoparticles have a higher absorption coefficient in the 350 -700 nm optical wavelength range. The solar cell device was modeled and simulated under the Standard Test Conditions (STC) of AM 1.5 G, 100 mW/cm2, and temperature of 300K. The summary of material properties or parameters that have been applied in this work is clearly shown in Table 1 and Table 2 for CuO, ZnO and AZO layers, including the front and back contacts. The main functionality of SCAPS-1D software is to find the solution by solving the one-dimensional semiconductor equations. Equation 1 describes the solution that is applied in SCAPS-1D in the bulk case of the layers,

$$\frac{\partial}{\partial x} = \varepsilon_0 \varepsilon \frac{\partial \Psi}{\partial x} = \frac{\partial^2 \Psi(x)}{\partial x^2} - q\left(p - n + N_D - N_A + \frac{\rho def}{q}\right) \quad (1)$$

where Ψ(x) is the electrostatic potential, p and n are electron and hole density respectively. ε_0 and ε are the vacuum and relative permittivity, respectively. ND and NA are the symbols for charged impurities of the donor and acceptor, and ρ signifies the electron/hole distribution.

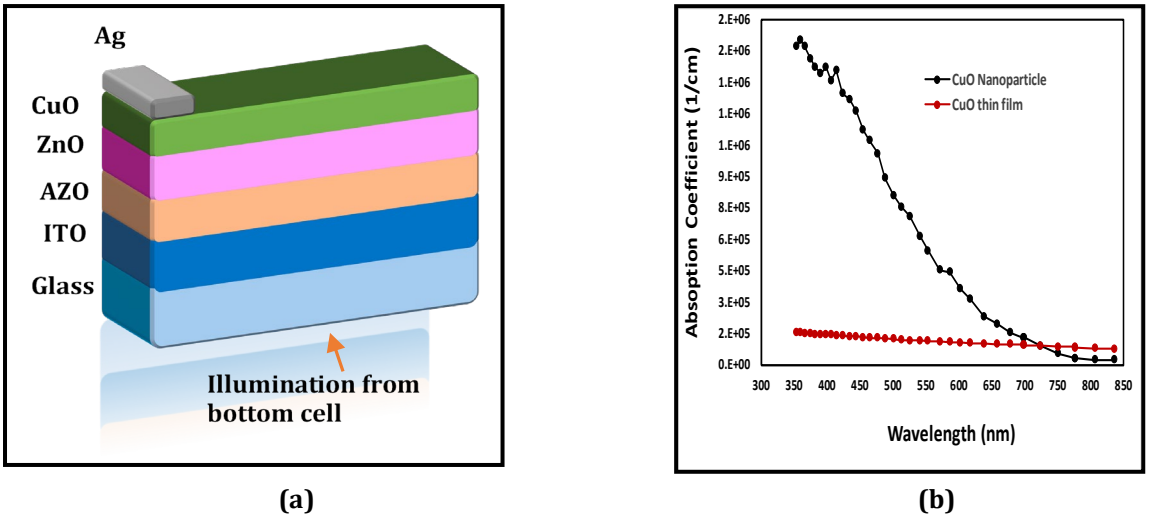

Fig. 1 *(a) CuO-based STFSC device structure simulated using SCAPS-1D; (b) The absorption coefficient of p-CuO thin film versus CuO plasmonic nanoparticles when used as the absorber layer in STFSC device*

Table 1 *Parameters of ZnO, CuO, and AZO used in SCAPS-1D simulation*

Parameters	i-ZnO	p-CuO	AZO
Thickness (nm)	10-300	10-110	200
Bandgap (eV)	3.400	1.5	3.300
Electron Affinity (eV)	4.1	4.070	4.450
Dielectric Permittivity (Relative)	10	18.100	9
CB Effective Density of States (1/cm^3)	4.0x10^{18}	2.2x10^{19}	2.2x10^{18}
VB Effective Density of States (1/cm^3)	9.0x10^{18}	5.5x10^{20}	1.8x10^{19}
Electron Thermal Velocity (cm/S)	1.0x10^7	1.0x10^7	1.0x10^7
Hole Thermal Velocity (cm/S)	1.0x10^7	1.0x10^7	1.0x10^7
Electron Mobility (cm^2/Vs)	5.0x10^1	1.0x10^2	1.0x10^2
Hole Mobility (cm^2/Vs)	2.0x10^1	1.0x10^{-1}	2.5x10^1
Shallow Uniform Donor Density ND (1/cm^3)	5.0x10^{16}	0	1.0x10^{18}
Shallow Uniform Acceptor Density NA (1/cm^3)	0	1.0x10^{16}	1

Table 2 *Parameters of back and front contacts used in SCAPS-1D simulation*

Interface Parameters	Front Contact	Back Contact
Metal work function (eV)	4.472	5.297
Surface recombination velocity of holes (cm.s-1)	10^7	10^7
Surface recombination velocity of electrons (cm.s-1)	10^7	10^7

2.2 Taguchi Optimization

The developed STFSC device was optimized using Taguchi L9 method. This method was also used to define the order of importance of the control factors or parameters. It was also used to determine the effective parameter on the device structure and the best level of each parameter. As mentioned previously, Taguchi method consists of an orthogonal array, signal-to-noise ratio (S/N or SNR), and the response table and response graph (Main Effect Analysis (MEA). After the number of levels and the signal factors were determined, the experiments were executed. Output values of each experiment in the orthogonal array column were then converted to S/N. The mean

effective plot/response graph for S/N was plotted using optimum control factors for each output performance in the response table. The S/N can be analyzed using three performance characteristics: larger-the-better, nominal-the-better, and smaller-the-better [24]. In this work, the output characteristics of open circuit voltage (Voc), short circuit current (Jsc), fill factor (FF) and efficiency (η) used S/N of larger-is-better. Equation 2 provides the S/N calculation for larger-the-better characteristics.

$$Larger - the - better\ S/N = -10log10_{10}\left[\frac{1}{n}\sum_{i==1}^{n}\left(\frac{1}{Y_i^2}\right)\right] \quad (2)$$

where n the number of control factors and Yi denotes the results of the i-th turn of a set of n simulated trials. The four control factors for the STFSC were identified as the thickness of CuO absorber layer (Factor A), the doping concentration of CuO absorber layer (Factor B), the thickness of ZnO buffer layer (Factor C), and the doping of the ZnO buffer layer as the final factor (D). These factors have a profound effect on the performance of the STFSC device model. The four control factors and the assigned three levels with their values are summarized in Table 3.

Table 3 *Control factors and their level values used in the Taguchi L9 optimization method*

Symbol	Control Factors	Level		
		1	2	3
A	CuO thickness (nm)	50	80	110
B	CuO doping ($1/cm^3$)	$5e^{13}$	$5e^{15}$	$1e^{16}$
C	ZnO thickness (nm)	10	150	300

Next, analysis of variance (ANOVA) was used to show the relationship between the control factors and the four quality output characteristics. ANOVA consists of the degrees of freedom, sum of squares of control factors, variance of control factors, F-ratio of control factors, and the percentage contribution of control factors towards the output characteristics. Previous work reported an ANOVA significance of control factors quantified using a confidence level of 95 or 99 [25], and ANOVA uses the obtained data of S/N from orthogonal arrays in the Taguchi method.

3. Results and Discussion

Table 4 illustrates the summarized simulation calculations of the electrical and optical parameters for all 9 experiments. The calculated Voc range was 0.5539-0.714 V, while the JSC range was 10.2368-14.889 ($mA/cm^{2)}$. The results indicated that the electrical parameters of the CuO thin film-based STFSC devices crucially depend on the factors (thickness and doping) level of the CuO and ZnO thin films. On the other hand, the calculated FF were in the range of 44.51-82.27%, while the efficiency (η) was in the range of 3.49-9.92%.

Table 4 *Simulation plan and output characteristics of L9 Taguchi Method for CuO thin film-based STFSC device optimization*

Exp. number	Factor Level Values				Voc (V)	Jsc (mA/cm)	FF (%)	η (%)
	1	2	3	4				
1	50	$5e^{13}$	10	$5e^{13}$	0.5539	10.594975	75.78	4.45
2	50	$5e^{15}$	150	$5e^{16}$	0.6749	10.236812	78.42	5.42
3	50	$1e^{16}$	300	$5e^{18}$	0.6782	10.801147	82.27	6.03
4	80	$5e^{13}$	150	$5e^{18}$	0.5564	14.889223	79.25	6.57
5	80	$5e^{15}$	300	$5e^{13}$	0.7140	10.983167	44.51	3.49
6	80	$1e^{16}$	10	$5e^{16}$	0.7	14.719729	76.87	8.02
7	110	$5e^{13}$	300	$5e^{16}$	0.5762	17.295531	77.27	7.70
8	110	$5e^{15}$	10	$5e^{18}$	0.6874	17.893431	80.67	9.92
9	110	$1e^{16}$	150	$5e^{13}$	0.7399	16.074557	59.14	7.03

Int. Journal of Integrated Engineering Vol. 16 No. 9 (2024) 264-272

Fig. 2 (a)-(d) shows the response graph of the S/N ratio towards the four control factors at each level for each output characteristic VOC, JSC, FF and efficiency (η). The larger the S/N ratio, it reflects a better performance for STFSC device optimization. For Voc, the best combination of control factors was A3B3C3D1. For JSC, the best combination of control factors is A3B1C1D3. For FF, the best combination of control factors is A1B1C1D3. And finally, for η, the best combination of control factors is A3B3C1D3. Since the best factor for each output differs from one another, the value of the S/N is used to find the best set of control factors. Else than that, the factor effect percentage can also be used to determine the best set of control factors.

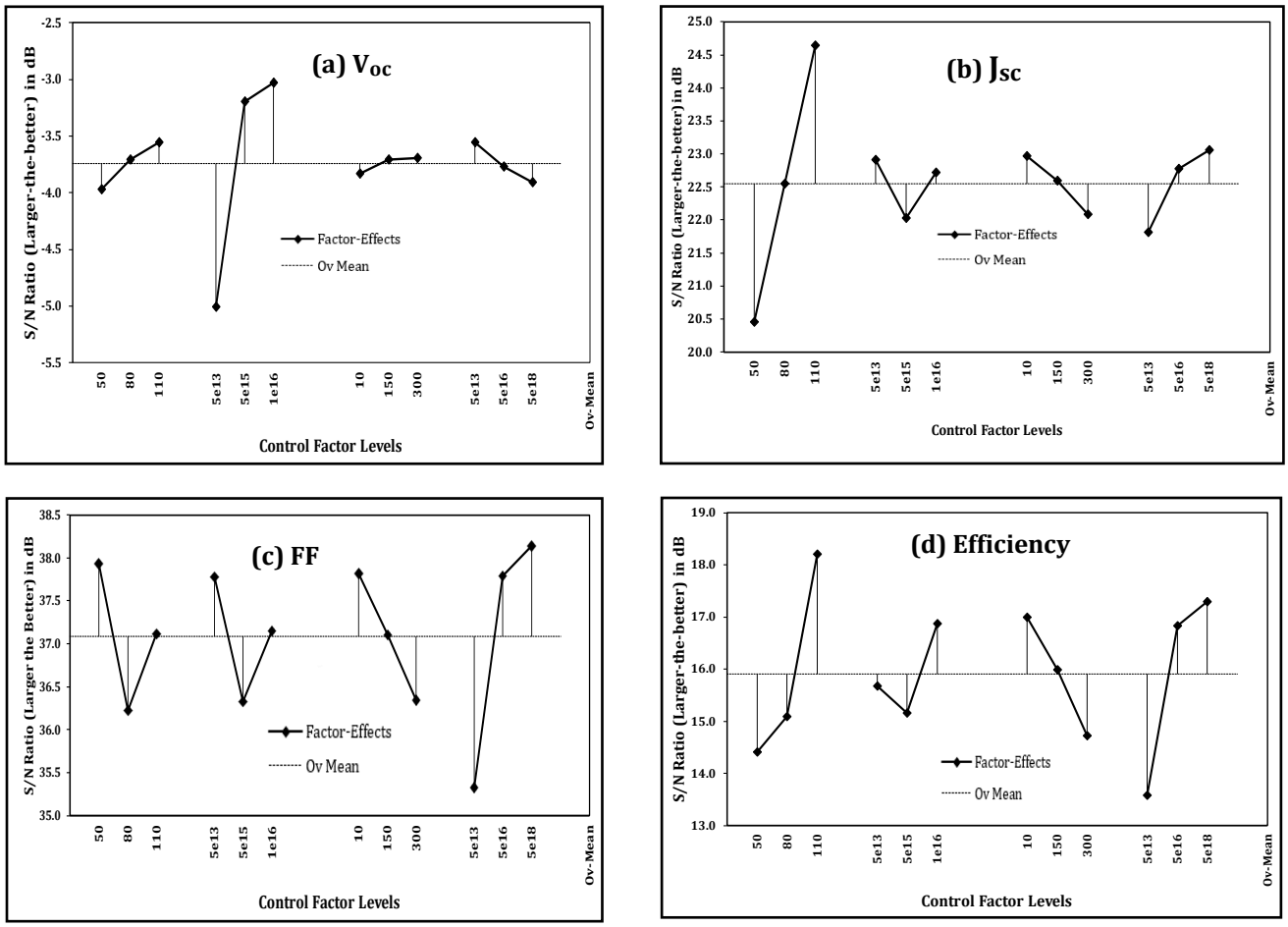

Fig. 2 *The Taguchi S/N response graph for CuO-based STFSC device for all the output characteristic (a) Voc; (b) Jsc; (c) FF; and (d) η*

The output response in terms of control factor effect on the S/N ratio for CuO thin film-based STFSC device is presented in Table 5, where the S/N ratio was calculated using "Larger-the-better" output characteristics for Voc, Jsc, FF, and η. The larger the S/N ratio and factor effect percentages, it reflects a better performance for device optimization. According to the results, for better Voc performance, factor B (CuO thin film doping) at level 3 ($1e^{16}$ /cm^3) is the dominant factor with factor effect of 94 %, followed by Factor A (CuO thin film thickness) at level 1 (50 nm) with factor effect of 4 %. Factor B has a greater significance in providing a better Voc performance, followed by Factor A. Factor D and C have low factor effect percentages on the Voc performance and hence are not crucial.

In terms of the Jsc performance, Factor A at level 3 (110 nm CuO thin film thickness) has the highest S/N factor effect at 84%, followed by factor D with an S/N percentage of 8%. Factor B and factor C affects the Jsc with 4% only. The fill factor (FF) shows that the highest factor effect percentage comes from Factor D at 57% at Level 3 (ZnO doping at 5e18 /cm3) followed by Factor A (18%), Factor B (13%) and Factor C (13%). Finally, for better efficiency (η) performances, factor A and factor D are the dominant S/N with factor effect of 40%. This is followed by Factor C (13%) and Factor B (8%). Therefore, the best combination of control factors is A3B3C1D3 which is equivalent to CuO thin film thickness of 110 nm (A3) with doping concentration of $1e^{16}$ /cm3 (B3) and ZnO thin film thickness of 10 nm (C1) with doping concentration of 5e18 /cm3 (D3).

Fig. 3 compares the J-V curves of two types of CuO-based STFSC; one utilizing thin film CuO layer as the absorber layer and another utilizing CuO plasmonic nanoparticles as the absorbing layer. The CuO thin film-based device has a lower photocurrent than CuO nanoparticle-based device. The result indicate that CuO nanoparticle-

based device provides a higher Jsc value of 456.78 mA/cm2 and Voc value of 0.75 V. In comparison, the Jsc and Voc values are 276.87 mA/cm2 and 0.77 V, where the Jc value is much lower in the CuO thin film-based devices. Based on the results obtained, it is concluded that utilization of CuO plasmonic nanoparticles as the absorbing layer in STFSC device provides a larger surface area for light absorption and subsequently higher current generation due to the higher absorption coefficient as portrayed in Fig 1(b).

Table 5 *The calculated S/N response of control factors with optimal parameters*

Control Factor	Voc (V)		Jsc (mA/cm)		FF (%)		η (%)		Optimal Parameter
	Level	% Factor Effect	Level	% Factor Effect	Level	% Factor Effect	Level	% Factor Effect	
A	1	4	3	84	1	18	3	40	A3
B	3	94	2	4	1	13	3	8	B3
C	1	0	2	4	1	13	1	13	C1
D	3	2	3	8	3	57	3	40	D3

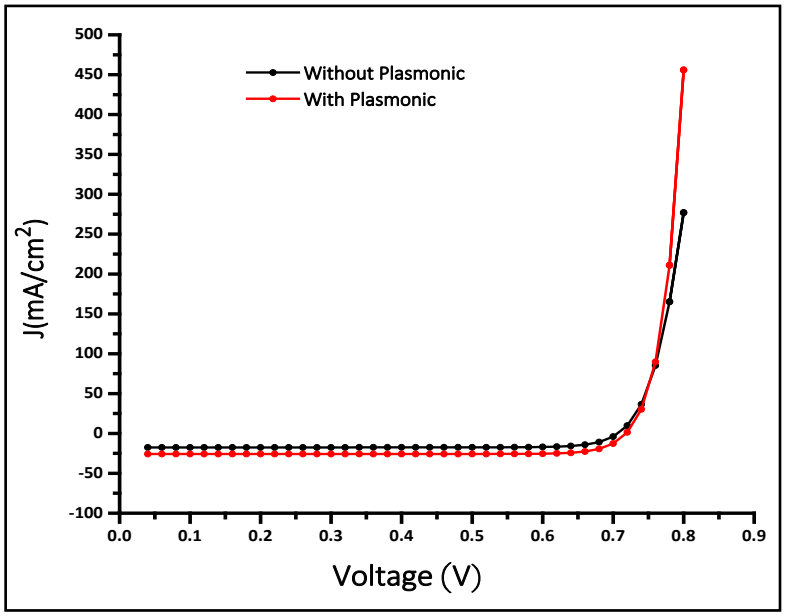

Fig. 3 *J–V curves of STFSC comparing absorber layers using thin film-based CuO layer versus CuO plasmonic nanoparticle-based devices*

Table 6 compares the Taguchi optimization of the output characteristics of the CuO-based STFSC utilizing CuO thin film (A3B3C1D3) versus CuO nanoparticles as the absorber layer. It clearly indicates that all output parameters show increased values when CuO nanoparticles are used as the absorbing layer. The Voc improves by 1.64%, the JSC improves by 46%, the FF improves by 1.77% and finally the efficiency improves by 51% when CuO nanoparticles are used as the absorbing layer in STFSC device. The higher surface area of CuO nanoparticles allow a larger amount of light to be absorbed hence increasing the amount of current generated in the STFSC device.

Table 6 *L9 Taguchi optimization and comparison between CuO thin film and CuO plasmonic nanoparticle-based absorber layers in the STFSC device*

Materials	A (nm)	B ($1/cm^3$)	C (nm)	D ($1/cm^3$)	V_{OC} (V)	J_{SC} (mA/cm)	FF (%)	η (%)
CuO thin film	110	$1e^{16}$	10	$5e^{18}$	0.7068	17.566	82.735	10.273
CuO nanoparticles	110	$1e^{16}$	10	$5e^{18}$	0.7184	25.734	84.20	15.566

Int. Journal of Integrated Engineering Vol. 16 No. 9 (2024) 264-272

Fig. 4 exhibits the quantum efficiency (QE) comparison between both STFSC devices utilizing CuO thin film and CuO plasmonic nanoparticles as the absorber layer. The CuO nanoparticle-based device records a QE value ~90% across the visible wavelengths ranging from 350 to 800 nm whereas the QE value of the CuO thin film-based device was recorded at ~60%; an increase of 50%. The improvement clearly shows the presence of the plasmonic /nanoparticles effect on the structure of the device, in which the nanoparticles absorb more photons and generates higher current density.

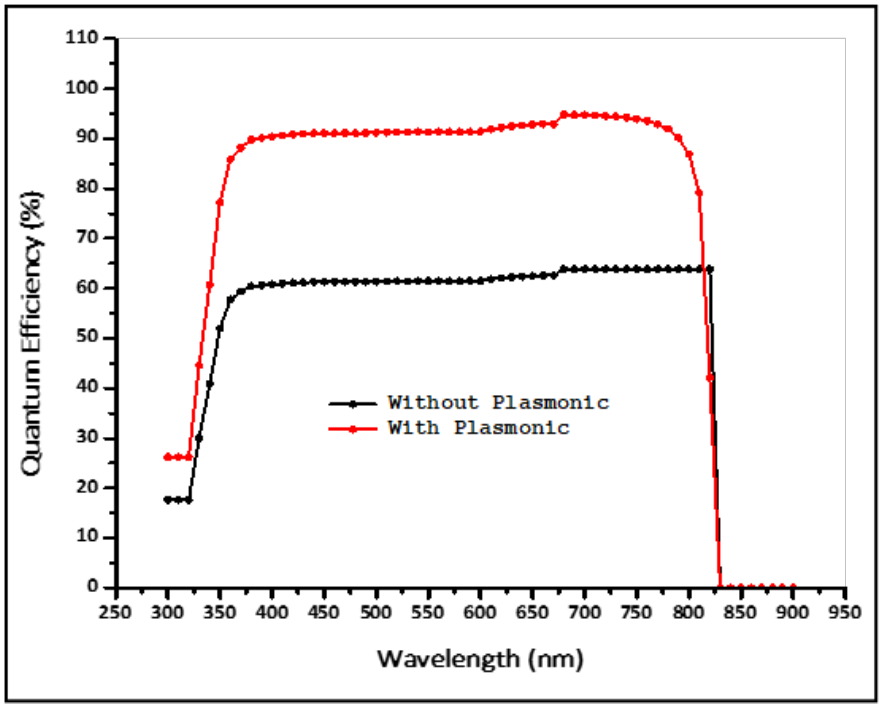

Fig. 4 *Quantum Efficiency (QE) comparison between STFSC devices with and without plasmonic CuO nanoparticles as the absorber layer*

4. Conclusion

The L9 Taguchi orthogonal array and ANOVA methods were applied to obtain optimized control factor parameters, such as the best thickness and doping levels that enhance the performance of CuO thin-film/CuO nanoparticle-based STFSC devices. As a result, the best combination of control factors is A3B3C1D3 which is equivalent to CuO thin film thickness of 110 nm (A3) with doping concentration of 1e16 /cm3 (B3) and ZnO thin film thickness of 10 nm (C1) with doping concentration of 5e18 /cm3 (D3). This gives the output parameters of VOC of 0.7068 V, JSC is 17.566 mA/cm, fill factor achieved 82.735 % and the efficiency was 10.273 %. In addition, replacement of the CuO thin film with CuO nanoparticles as the absorber layer further enhanced all device output parameters from a minimum of 1.64% to 51% in terms of increment percentage. Therefore, a plasmonic CuO-nanoparticle-based STFSC device achieved efficiency of 15.57%. The effect of nanoparticles or plasmon polaritons that propagate in the plane of the semiconductor thin film layer is beneficial, and extremely thin photovoltaic absorber layers (tens to hundreds of nanometres thick) are capable of absorbing photons from the entire solar spectrum. This can confine light excessively, increase the photocurrent and consequently, improve the PCE conversion.

Acknowledgement

We acknowledge the technical support from the Institute of Microengineering and Nanoelectronics (IMEN) and Solar Energy Research Institute (SERI), UKM. This research was funded in part by the International Grant RR-2023-006. This publication is also an outcome of the R&D work undertaken by the ASEAN-India Collaborative R&D scheme under the ASEAN-India S&T Development Fund (AISTDF) by DST-SERB, Govt. of India (Grant Nos. IMRC/AISTDF/CRD/2018/ 000068 and RR-2020-002).

Conflict of Interest

Authors declare that there is no conflict of interests regarding the publication of the paper.

Author Contribution

The authors confirm contribution to the paper as follows: ***study conception and design:*** *JH, PC, PSM;* ***data collection:*** *JH, PC, PSM;* ***analysis and interpretation of results:*** *JH, PC, PSM;* ***draft manuscript preparation:*** *JH, PC, PSM, NAJ, KSS, TRL, HK, MAM, ARZ and JS. All authors reviewed the results and approved the final version of the manuscript.*

References

[1] Issam Khele, Márta Szabó (2024) A review of the effect of semi-transparent building-integrated photovoltaics on the visual comfort indoors, *Developments in the Built Environment, Volume 17,100369, ISSN 2666-1659,* https://doi.org/10.1016/j.dibe.2024.100369.

[2] Abdelfatah M, El Sayed AM, Ismail W, Ulrich S, Sittinger V, El-Shaer A. (2023) SCAPS simulation of novel inorganic ZrS2/CuO heterojunction solar cells. *Sci Rep. Mar 20;13(1):4553*, https://doi: 10.1038/s41598-023-31553-4. PMID: 36941320; PMCID: PMC10027670.

[3] H. Siddiqui, M. Qureshi, and F. Z. Haque (2016) Valuation of copper oxide (CuO) nanoflakes for its suitability as an absorbing material in solar cells fabrication, *Optik, vol. 127, no. 8, pp. 3713-3717,* https://doi.org/10.1016/j.ijleo.2015.12.133

[4] S. Ahmmed, A. Aktar, S. Tabassum, M. H. Rahman, M. F. Rahman, and A. B. M. Ismail (2021) CuO based solar cell with V2O5 BSF layer: Theoretical validation of experimental data, *Superlattices Microstructures, vol. 151, p. 106830,* https://doi.org/10.1016/j.spmi.2021.106830

[5] S. Dolai, R. Dey, S. Hussain, R. Bhar, and A. K. Pal (2019) Photovoltaic properties of F: SnO2/CdS/CuO/Ag heterojunction solar cell, *Materials Research Bulletin, vol. 109, pp. 1-9*, https://doi.org/10.1016/j.materresbull.2018.09.022

[6] G. Welegergs, H. Gebretnisae, M. Tsegay, Z. Nuru, S. Dube, and M. Maaza (2021) Thickness dependent morphological, structural and optical properties of SS/CuO nanocoatings as selective solar absorber *Infrared Physics Technology, vol. 113, p. 103619*, https://doi.org/10.1016/j.infrared.2020.103619

[7] A. Bhaumik, A. Haque, P. Karnati, M. Taufique, R. Patel, and K. Ghosh (2014) Copper oxide based nanostructures for improved solar cell efficiency, *Thin Solid Films, vol. 572, pp. 126-133*, https://doi.org/10.1016/j.tsf.2014.09.056

[8] M. Dahrul and H. Alatas (2016) Preparation and optical properties study of CuO thin film as applied solar cell on LAPAN-IPB Satellite, *Procedia Environmental Sciences, vol. 33, pp. 661-667,* https://doi.org/10.1016/j.proenv.2016.03.121

[9] R. Bunea, A. K. Saikumar, and K. Sundaram (2021) A comparison of optical properties of CuO and Cu2O thin films for solar cell applications, *Materials Sciences Applications, vol. 12, no. 7, pp. 315-329,* https://doi.org/10.4236/msa.2021.127021

[10] G. Wisz et al. (2021) Solar cells based on copper oxide and titanium dioxide prepared by reactive direct-current magnetron sputtering, *Opto-Electronics Review, vol. 29,* http://dx.doi.org/10.24425/opelre.2021.139039

[11] Y. H. Ribeiro, J. d. S. Pereira, D. G. David, and M. V. da Silva (2022) Growth, characterization, and photovoltaic application of copper oxide thin films, *Thin Solid Films, vol. 757, p. 139381,* https://doi.org/10.1016/j.tsf.2022.139381

[12] J. Husna, P. S. Menon, P. Chelvanathan, M. Mohamed, S. Tripathy, and T. Lenka (2021) Numerical study of semi-transparent thin film heterojunction p-CuO/n-ZnO/AZO/ITO solar cells device model using SCAPS-1D, *Chalcogenide Letters, vol. 18, no. 11,* http://dx.doi.org/10.15251/CL.2021.1811.667

[13] S. Sinha, D. K. Nandi, P. S. Pawar, S.-H. Kim, and J. Heo (2020) A review on atomic layer deposited buffer layers for Cu (In, Ga) Se2 (CIGS) thin film solar cells: Past, present, and future, *Solar Energy, vol. 209, pp. 515-537,* https://doi.org/10.1016/j.solener.2020.09.022

[14] A. Lakshmanan, Z. C. Alex, and S. Meher (2022) Recent advances in cuprous oxide thin film-based photovoltaics, *Materials Today Sustainability, vol. 20, p. 100244.* https://doi.org/10.1016/j.mtsust.2022.100244

[15] P. Sawicka-Chudy, M. Sibiński, G. Wisz, E. Rybak-Wilusz, and M. Cholewa (2018) Numerical analysis and optimization of Cu2O/TiO2, CuO/TiO2, heterojunction solar cells using SCAPS, *Journal of Physics: Conference Series, 2018, vol. 1033, p. 012002: IOP Publishing,* https://doi.org/10.1088/1742-6596/1033/1/012002

[16] P. Mahajan, A. Singh, and S. Arya (2020) Improved performance of solution processed organic solar cells with an additive layer of sol-gel synthesized ZnO/CuO core/shell nanoparticles, *Journal of Alloys Compounds, vol. 814, p. 152292,* https://doi.org/10.1016/j.jallcom.2019.152292

[17] D. H. Shin and S.-H. Choi (2018) Recent studies of semi-transparent solar cells, *Coatings, vol. 8, no. 10, p. 329,* https://doi.org/10.3390/coatings8100329

[18] H. Absike et al. (2021) Synthesis of CuO thin films based on Taguchi design for solar absorber, *Optical Materials, vol. 118, p. 111224,* https://doi.org/10.1016/j.optmat.2021.111224
[19] G. Taguchi (1987) System of experimental design; engineering methods to optimize quality and minimize costs, https://www.sidalc.net/search/Record/KOHA-OAI-TEST:13480/Description
[20] M. Pilor et al. (2021) The Use of Taguchi Method to Elaborate Good ZnO Thin Films by Sol Gel Associated to Dip Coating, *Int. J. Mater. Sci. Appl., vol. 10, no. 1, p. 18,* https://doi.org/10.11648/j.ijmsa.20211001.14
[21] H. Köçkar, N. Kaplan, A. Karpuz, and Ö. Karaağac (2023) Improvement of saturation magnetization of sputtered Fe/Al multilayer thin films using Taguchi Method supported by ANOVA, response surface methodology and regression analysis, *Acta Physica Polonica A, vol. 143, no. 5,* https://doi.org/10.12693/APhysPolA.143.381
[22] Y. Nouri et al. (2022) Synthesis of tin monosulfide SnS thin films via spray pyrolysis method based on Taguchi design for solar absorber, *Optical Materials, vol. 131, p. 11266,* https://doi.org/10.1016/j.optmat.2022.112669
[23] G.S. Mei, N.R.B. Mohamad, N.A.B. Jamil, B.Y. Majlis, P.S. Menon (2018) Optimization of Kretschmann based on surface plasmon resonance sensor using Taguchi method | Pengoptimuman sensor resonans plasmon permukaan berdasarkan kretschmann dengan Kaedah Taguchi, *Sains Malaysiana, 47(10), pp. 2565–2571,* http://dx.doi.org/10.17576/jsm-2018-4710-33
[24] J. Satpute et al. (2024) Performance optimization for solar photovoltaic thermal system with spiral rectangular absorber using Taguchi method, *Scientific Reports, vol. 14, no. 1, p. 23849,* https://doi.org/10.1038/s41598-024-73065-9
[25] Y.-Y. Hong, A. A. Beltran Jr, and A. C. Paglinawan (2018) A robust design of maximum power point tracking using Taguchi method for stand-alone PV system, *Applied Energy, vol. 211, pp. 50-63,* https://doi.org/10.1016/j.apenergy.2017.11.041
[26] W. Fan, G. Kokogiannakis, and Z. Ma (2018) A multi-objective design optimisation strategy for hybrid photovoltaic thermal collector (PVT)-solar air heater (SAH) systems with fins, *Solar Energy, vol. 163, pp. 315-328,* https://doi.org/10.1016/j.solener.2018.02.014